Efficient Quantification by X-ray Photoelectron Spectroscopy and Thermogravimetric Analyses of the One-Pot Grafting of Two Molecules on the Surface of Iron Oxide Nanoparticles

Lionel Maurizi, Fadoua Sallem, Julien Boudon, Olivier Heintz, Harender Bisht, Frederic Bouyer, Nadine Millot

▶ **To cite this version:**

Lionel Maurizi, Fadoua Sallem, Julien Boudon, Olivier Heintz, Harender Bisht, et al.. Efficient Quantification by X-ray Photoelectron Spectroscopy and Thermogravimetric Analyses of the One-Pot Grafting of Two Molecules on the Surface of Iron Oxide Nanoparticles. Journal of Nanoscience and Nanotechnology, 2019, 19 (8), pp.4920-4929. 10.1166/jnn.2019.16796 . hal-02163532

HAL Id: hal-02163532

https://hal.science/hal-02163532

Submitted on 6 Nov 2020

HAL is a multi-disciplinary open access archive for the deposit and dissemination of scientific research documents, whether they are published or not. The documents may come from teaching and research institutions in France or abroad, or from public or private research centers.

L'archive ouverte pluridisciplinaire **HAL**, est destinée au dépôt et à la diffusion de documents scientifiques de niveau recherche, publiés ou non, émanant des établissements d'enseignement et de recherche français ou étrangers, des laboratoires publics ou privés.

Surface characterizations to quantify complex one-batch functionalization of iron oxide nanoparticles

Lionel Maurizi[1], Fadoua Sallem[1], Julien Boudon[1], Olivier Heintz[1], Harender Bisht[1], Frédéric Bouyer[1] and Nadine Millot[1*]*

[1]Laboratoire Interdisciplinaire Carnot de Bourgogne, UMR 6303, CNRS, Université Bourgogne Franche-Comté, BP 47870, 21078 Dijon Cedex, France

[*] *Corresponding authors: lionel.maurizi@u-bourgogne.fr and nmillot@u-bourgogne.fr*

Abstract

Superparamagnetic iron oxide nanoparticles (SPION) can be developed for biomedical applications but need to be functionalized before use to avoid agglomeration in biological media. In this study, SPION were functionalized in one step with two organic molecules. Firstly, polyethylene glycol (PEG) was mixed for 46 hours to improve steric stability and then, two hours before the end of the reaction, dimercaptosuccinic acid (DMSA) was added to provide negative charges and thiol groups. Three different molecular weights of PEG were used (550, 2000 and 5000 $g.mol^{-1}$). We demonstrated that by coupling thermogravimetric to X-Ray photoelectron spectrometry analyses it was possible to quantify accurately the covering of SPION's surface. We also showed that the length of the PEG influenced the quantity of DMSA adsorbed. With the smallest PEG (550 $g.mol^{-1}$) the presence of DMSA is almost ten times higher than with the two other PEG used proving that long polymers prevent the adsorption of small molecules on the surface of SPION.

Keywords: SPION, quantification of organic molecules, XPS, TGA, surface, grafting

Introduction

Superparamagnetic iron oxide nanoparticles (SPION) are developed for several biological applications such as hyperthermia, drug delivery or Magnetic Resonance Imaging (MRI) [1-5]. To have the superparamagnetic properties, iron oxide nanoparticles should crystallize in a spinel structures (AB_2O_4) like Fe_3O_4 (magnetite) or γ-Fe_2O_3 (maghemite) [6, 7] and have a particles size smaller than 20 nm [8]. The major limit of the use of SPION in biomedical applications is their poor colloidal stability in physiological conditions. In order to avoid the particles agglomeration, chemical modifications of their surface are usually used.

Two types of stabilization are commonly used to enhance nanoparticles stability; electrostatic and steric. The first type uses an electrostatic stabilizing agent that provides a negative or a positive charge onto particles surface and stabilizes them by repulsive electrostatic forces. Carboxylic acids [9-11] or phosphates groups [12, 13] are examples of stabilizing agents which were used to provide a negative electrostatic stability for SPION. They can be grafted directly onto the surface by chelating interactions between SPION's hydroxyl groups and carboxyl and phosphate functions [14].

The second type is the steric stabilizing agents. The commonly used are polymers with long hydrophilic chains. They stabilize nanoparticles by steric repulsions at physiological conditions [15, 16]. However, the grafting of steric stabilizing agent onto nanoparticles surface needs a pre-functionalization step with linking molecules. This step avoids SPION's cross-linking which increases drastically their size and consequently decreases their colloidal stability. Organosilane molecules such as aminopropyltriethoxysilane (APTES) or isocyanatopropyltriethoxysilane (ICPTES) are potential linker molecules used for covalent grafting of polymers, proteins or antibodies onto iron oxide nanoparticles [17, 18].

Ones functionalized, the obtained nanohybrids should be characterized to determine the coverage percentage of organic matter on the inorganic core. Classical used methods are

Thermogravimetric analysis (TGA), Infrared Spectroscopy (FITR) or Zeta potential measurements. They can give an estimation of the presence of molecules on the surface of iron oxide. X-ray Photoelectron spectroscopy (XPS) is also a useful method to get an atomic concentration of different species in complex chemistry systems [12, 19-24].

This work discusses the one step functionalization of SPION, in one batch, with both DMSA (Dimercaptosuccinic acid) and $mPEG_x$-Si polymers (silanated-methoxyPolyEthyleneGlycol, where x = 550, 2000 and 5000 $g.mol^{-1}$). DMSA was used as electrostatic stabilizing agent and in the same time gives thiol functions useful for further functionalization. It has interesting features as biocompatible property, not expensive and simple to use [10, 25]. As PEG could not be covalently linked to SPION surface, silanated-PEGs, with different length chain, were chosen as steric stabilizing agents [17, 26].

The obtained functionalized SPION were then characterized with several techniques which are TGA, FTIR and Zeta potential measurements to highlight the chemical interactions happened between the organic molecules and SPION. XPS elementary analysis was also carried out to better understand the type of elaborated bonds at nanohybrids surface. Thanks to XPS it was possible to illustrate the presence of grafted molecules onto iron oxide's surface through the decomposition of the peaks in the spectra and prove the importance of polymers length chain on the surface covering.

Materials and methods

Reagents

Iron (II) chloride tetrahydrate ($FeCl_2.4H_2O$), iron (III) chloride hexahydrate ($FeCl_3.6H_2O$), sodium hydroxide (NaOH), hydrochloric acid (HCl 37%), nitric acid (HNO_3 69%), meso-2,3-dimercaptosuccinic acid (DMSA), methoxy-PEG (molecular weight 550, 2000 and 5000 $g.mol^{-1}$), 3-isocyanatopropyltriethoxysilane (ICPTS), dibutyltin dilaurate (DBTL), *n*-hexane and tetrahydrofuran (THF) were purchased from Aldrich and used without any further purification. THF was distilled over sodium metal and benzophenone just before use.

Nanoparticles preparation

Magnetic core preparation:

Naked SPION were synthesized following a classical co-precipitation protocol [23, 27, 28]. Briefly a stoichiometric mixture of 20 mL of iron (II) chloride solution (2M) and 80 mL of iron (III) chloride solution (1M) (molar ratio Fe^{II}:Fe^{III} = 1:2) was added dropwise to 800 mL of 0.75 M NaOH solution (25°C). The basic SPION suspension is then washed 7 times and peptized with HNO_3 solution (1M) and water. The final suspension is then dialyzed for 24 hours against pH 3 HNO_3 solution. The obtained suspension was kept at pH 3 with a mass concentration of SPION of 23 mg.mL^{-1}.

mPEG-Si synthesis:

Silanated-methoxy-PEGs (mPEG-Si) are obtained by the reaction of 3-isocyanatopropyltriethoxysilane (ICPTS) with methoxy-PEG (550, 2000 and 5000 g.mol^{-1}) [29] in dried tetrahydrofuran (THF), at 60°C, under nitrogen flow, for 48 hours and using dibutyltindilaurate as catalyst. The synthesized mPEG$_x$-Si products (x = 550, 2000 and 5000 g.mol^{-1}) were finally precipitated in hexane.

Nanohybrids preparation:

SPION functionalizations with mPEG-Si and DMSA (mPEG$_x$-SPION-DMSA where x = 550, 2000, 5000 g.mol^{-1}) were carried out as mentioned in our previous work [30]. Briefly, 0.13 mmol of mPEG-Si were dissolved in 40 mL of ethanol/water (50/50: v/v [29, 31, 32]) at 25°C and pH 4. Then, 100 mg of SPION were added to the mixture and stirred for 48 hours under nitrogen gas. Two hours before the end of the reaction, 0.0439 mmol of DMSA were added to the suspension. The modified SPION are then washed by dialysis against water for one week.

Parts of the obtained suspensions were freeze-dried for 48 hours and the dried powders were finally characterized. The rest of the suspension is conserved in acidic conditions.

Characterization

X-ray powder diffraction patterns were recorded using a Siemens D5000 diffractometer with Cu K_{β} at λ=1.3922 Å for 48 hours which gives lattice parameter and crystallite's mean size using Topas software [33]. Correction for instrumental broadening was determined from a standard reference material.

Zeta potential measurements were carried out with Malvern zetasizer using DTS Nano 4.20 software, in the range of pH between 3 to 11. The nanoparticles suspensions were diluted to approximately 200 $\mu g.mL^{-1}$ in 10^{-2} M NaCl solution. The NaCl stock solution was previously filtered through 0.8 µm filter. The suspensions pH were adjusted with HCl 10^{-1} M and NaOH 10^{-1} M solutions.

Fourier Transformed InfraRed (FTIR) measurements were recorded on a Bruker IFS 28 apparatus using OPUS version 3.1. Pellets composed of 2 mg of dried samples and 198 mg of KBr were made. The step of analysis was 2 cm^{-1}.

Surface area measurements were performed using a BELSORP-mini apparatus with N_2 gas adsorption. The BET method was used in the calculation of surface area values (S_{BET}) from the isotherm of nitrogen adsorption.

Samples decomposition as well as the coverage percentage of grafted molecules onto particles surface were studied by thermogravimetry (SETARAM TAG24). This symmetric thermobalance was able to measure weight variations of 0.1 µg. The heating rate was 2°C.min^{-1} up to 800°C under N_2/O_2 flow ((0.12 : 0.04) L/min). Sample weights were around 5 to 10 mg.

XPS analyses were performed by a SIA 100 Riber/Cameca apparatus and a monochromated Al Kα X-ray source (energy of 1486.6 eV, accelerating voltage of 12 kV and power of

200 W) [34]. A Riber Mac 2 semi-imaging spectrometer was used with a resolution (measured from the Ag 3d5/2 line width) of 2.0 eV for global spectra and 1.3 eV for windows corresponding to selected lines. The spectrometer was used with its axis perpendicular to the surface of the sample. Samples were prepared by deposition of the powders on an indium sheet of about 10 x 10 x 5 mm dimensions. Photoemission peak areas were calculated after smoothing and background subtraction using a Shirley routine. XPS spectra were decomposed into components according to Gaussian (70%)-Lorentzian (30%) profile peaks. In the fitting procedure, Full Width at Half Maximum (FWHM) were fixed between 1.5 and 2.0 eV except for the curves fitting of the N1s (2.0–2.3 eV) peaks.

<u>Results and discussions</u>:

Chemical and structural analyses of naked SPION:

It should be noted first that the XRD patterns (shown in supplementary information Figure SI1) corresponds to the spinel crystallographic phase of either magnetite (Fe_3O_4) or maghemite (γ-Fe_2O_3) with crystallite size around 8 nm. The lattice parameter of the SPION is a=8.37 Å, value between those of these two phases. Thanks to the Poix method [35], the lattice parameter can lead to the δ parameter (deviation from oxygen stoichiometry) in the formula $Fe_{3(1-\delta)}O_4$. With a= 8.37 Å, $\delta = 0.063$ and so the mean composition of the SPION nanocrystals is $Fe_{2.811}O_4$.

The surface area (S_{BET}) of naked SPION is 110 ± 1 $m^2.g^{-1}$. The calculated crystallite size from S_{BET} value is 11.2 ± 0.2 nm. This value is a little bit higher than that determined by XRD method (7.9 nm) due to the approximation made to the former method to relate the specific surface area and the particles diameter. The weight loss of dried SPION powder is 8.3% and their isoelectric point was at about pH 7.

XPS elementary analysis shows the presence of three elements which are iron (40% Fe2p), oxygen (56% O1s) and pollution carbon (4% C1s) summarized on Figure 1-a. The fit of O1s peak shows the presence of two components (Figure 1-b), located at 529.2 eV and 531.7 eV. The component peak situated at 529.2 eV is assigned to O^{2-} of spinel structure and that at 531.7 eV to OH surface groups with a relative proportion of 49% (87.5% of 56% O1s) and 7% (12.5% of 56% O1s) respectively.

a)

particles	Fe 2p (%)	O1s (%)	C1s(%)
Naked SPION	40	56	4

b)

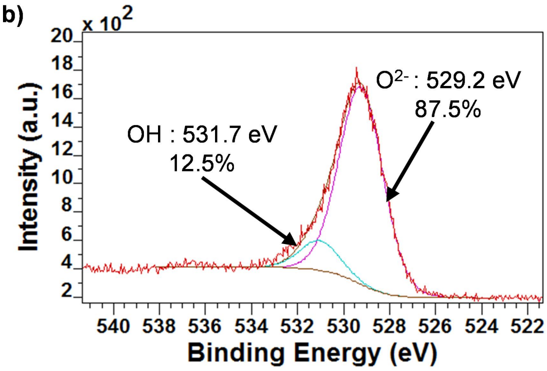

Figure 1: a): Atomic concentration of elements measured by XPS on naked SPION; b): Decomposition of O1s XPS spectrum of naked SPION

The experimentally calculated Fe/O ratio, obtained from XPS analysis, is equal to 0.71 (40%/56%). This value is in a good agreement with the theoretical value which is the average of Fe/O ratio in the stoichiometric proportions of Fe_3O_4 (0.75) and γ-Fe_2O_3 (0.67) and close to the ratio calculated from XRD results (0.70). This result proves that XPS is a reliable technique which gives accurate information about nanoparticles chemistry and their stoichiometry.

All of these standard results were used to compare SPION after surface modifications.

Characterization of molecules before their grafting:

DMSA and mPEG$_x$-Si (x = 550, 2000 and 5000 g.mol^{-1}) were characterized and used as references to be compared later to SPION modified surface. The semi developed formula of mPEG$_{2000}$-Si is given on the Figure 2. The average numbers of repeating units of the mPEG-Si (n in the formula on Figure 2) are 12, 43 and 112 for $mPEG_{550}$-Si, $mPEG_{2000}$-Si and $mPEG_{5000}$-Si respectively.

For DMSA, the weight loss in TGA (Figure SI2) is 98% however, for $mPEG_x$-Si the weight loss is proportional to the molecular weight of the polymer. Indeed, after the combustion of the mPEG-Si, silicon remains in silica form SiO_2 (M = 60 $g.mol^{-1}$). The relative percentage of SiO_2, compared to the total molecular weight of molecule, decreases with the increase of the length chain of polymer. The TGA weight loss for $mPEG_{550}$-Si, $mPEG_{2000}$-Si and $mPEG_{5000}$-Si are 92%, 98% and 99% respectively (Figure SI2). This result is in a good accordance with theoretical percentages which are 92.5%, 97.4% and 98.9% respectively.

Infrared specific vibration bands of each molecule were also identified before grafting to use them as a proof for SPION's grafting [36, 37] (Figure 2). The band located at 1700 cm^{-1} in DMSA spectrum is assigned to the stretch vibration band of carbonyl function ν COOH [38]. The mPEG-Si spectrum is the same for the three length chain polymers (550, 2000 and 5000), so only one is presented in Figure 2. The stretch vibration band of carbonyl function in this molecule is recorded at 1720 cm^{-1} [39]. This red shift can be explained by the difference in C=O environment which is surrounded by two nucleophilic atoms in carbamate bond (O=C-NH) and illustrates the successful linkage between the silane group of ICPTES and methoxy-PEG. The chemical bond between PEG and ICPTES is also proved by the presence of stretch vibration of N-H at 1500 cm^{-1} [39]. The stretch vibration of CH_2 in $mPEG_x$-Si is illustrated by the presence of a strong band at around 2900 cm^{-1}. However, a bending vibration band of C-H bond is recorded at 1420 cm^{-1}. The band situated at 2560 cm^{-1} in DMSA spectrum is assigned to the stretch of thiol S-H bond [40]. The intense band at about 1120 cm^{-1}, in mPEG-Si spectrum, is attributed to the stretching of C-O bond.

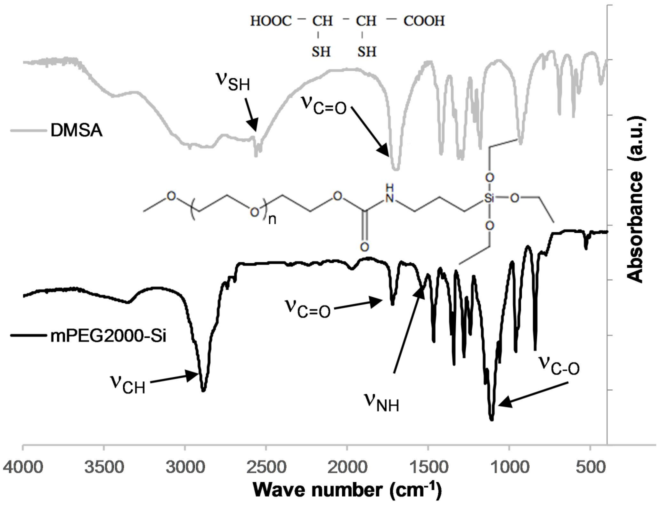

Figure 2: Semi-developed formula and FTIR spectra of meso-2,3-dimercaptosuccinic acid (DMSA) and silanated-methoxy-PEG$_{2000}$

XPS elementary analyses of non-grafted DMSA and mPEG$_x$-Si are presented in Table 1. This table shows the presence of three elements for DMSA which are carbon C1s (from 283 to 292 eV with a proportion of 43.8%), oxygen O1s (around 533 eV with a proportion of 38.9%) and sulfur S1s (around 164 eV with a proportion of 17.3%). The decomposition of carbon peak conduces to the determination of three components as shown in Figure SI3. DMSA is a symmetric molecule with four carbons where carbon atoms are grouped in pairs. The only two types of carbon thereby present should be components O-C=O and C-C-S in the C1s contribution. The third observed component at 284.5 eV is attributed to the pollution carbon C-C with a contribution of 5.5% of the total carbon percentage and 2.4 % of all elements. Since this type of carbon does not exist in DMSA, it is not taken into account and will be removed from the ratio calculation in this part. The C1s component peak at 286.3 eV has an important shift of about 1.5 eV from the conventional C-C bond position (284.8 eV). This shift is explained by the bonding of carbon to an element with higher electronegativity. In the case of DMSA, this element should be the sulfur. Consequently, this component is attributed to C-S bond with 53% of the total carbon percentage. Basing on the same reason, the C1s peak component situated at 289.5 eV is assigned to O-C=O bond with 41.5% of the total amount of carbon. The experimental proportion of these two components (56:44) is in a good correlation with the theoretical one (50:50). The O1s peak decomposition was not possible because DMSA molecule is symmetric and so oxygen atoms are equivalent (Figure SI3).

Taking into account all the previous observations, the experimental atomic percentages of the three elements was corrected as following: 42.4%, 39.9% and 17.7% for carbon, oxygen and sulfur respectively. These values are very close to the theoretical ones (40%, 40% and 20%) as shown in Table 1.

XPS analyses were also carried out for silanated methoxyPEG$_x$ with x = 550, 2000 or 5000 g.mol^{-1}. The results showed the presence of four elements which are carbon C1s (from 282.0 to 290.0 eV), oxygen O1s (from 528.0 to 536.0 eV), nitrogen N1s (around 299.0 eV) and silicon Si1s (around 102.0 eV). The decomposition of C1s and O1s peaks are given in supplementary information Figure SI3 and atomic percentages of the three measured polymers are summarized in Table 1. It is noted from the obtained results that the theoretical estimated percentages are similar to the XPS measured values. Given the large amount of carbon in the organic chain of mPEG$_x$-Si, the contribution of pollution carbon is neglected even for mPEG$_x$-SPION. Two new elements (nitrogen and silicon) appear in XPS analyses of mPEG$_x$-Si polymers. Nitrogen proves the presence of the carbamate bond which links mPEG to ethoxy-silane molecule. The atomic percentage of nitrogen is the same than that of silicon for the three polymers. Considering the chemical formula of the polymers, it is the proof that the carbamate bond is conserved.

It is to conclude from the previous elementary analyses of pure DMSA and mPEG$_x$-Si polymers that XPS could be a reliable method to characterize organic molecules and follow their grafting efficiency onto SPION’s surface.

Table 1: Theoretical and XPS measured atomic percentages of pure DMSA and mPEG$_x$-Si (where x = 550, 2000 or 5000 g.mol^{-1})

Element / Molecule	C1s		O1s		S1s		N1s		Si1s	
	Theo*	Exp§	Theo*	Exp§	Theo*	Exp§	Theo*	Exp§	Theo*	Exp§
DMSA	40.0	42.2	40.0	39.9	20.0	17.7	-	-	-	-
mPEG$_{550}$-Si	64.9	64.6	31.6	31.1	-	-	1.75	2.15	1.75	2.15
mPEG$_{2000}$-Si	66.0	66.2	31.7	31.8	-	-	0.65	1.1	0.65	0.9
mPEG$_{5000}$-Si	66.4	70.4	33.0	28.7	-	-	0.3	0.5	0.3	0.4

*Theoretical calculated value, §XPS measured value

Chemical analysis of elaborated nanohybrid: mPEG-Si-SPION-DMSA:

DMSA and mPEG$_x$-Si (x= 550, 2000 or 5000 g.mol^{-1}) modified SPION were analyzed using a large number of techniques as Zeta potential analysis, TGA, FTIR and XPS.

The isoelectric point (IEP) of elaborated mPEG$_x$-Si-SPION-DMSA nanohybrid shifted from 7 to less than 3 [2]. This shift proves a change in the global charge of nanoparticles surface. As the PEG is a neutral polymer that does not affect the global surface charge of nanoparticles, the noted change in charge is almost due to DMSA molecule and confirms its grafting. TGA results of the three functionalized SPION show weight losses of 31%, 56% and 78% for mPEG$_{550}$-Si-SPION-DMSA, mPEG$_{2000}$-Si-SPION-DMSA and mPEG$_{5000}$-Si-SPION-DMSA respectively (Figure SI4).

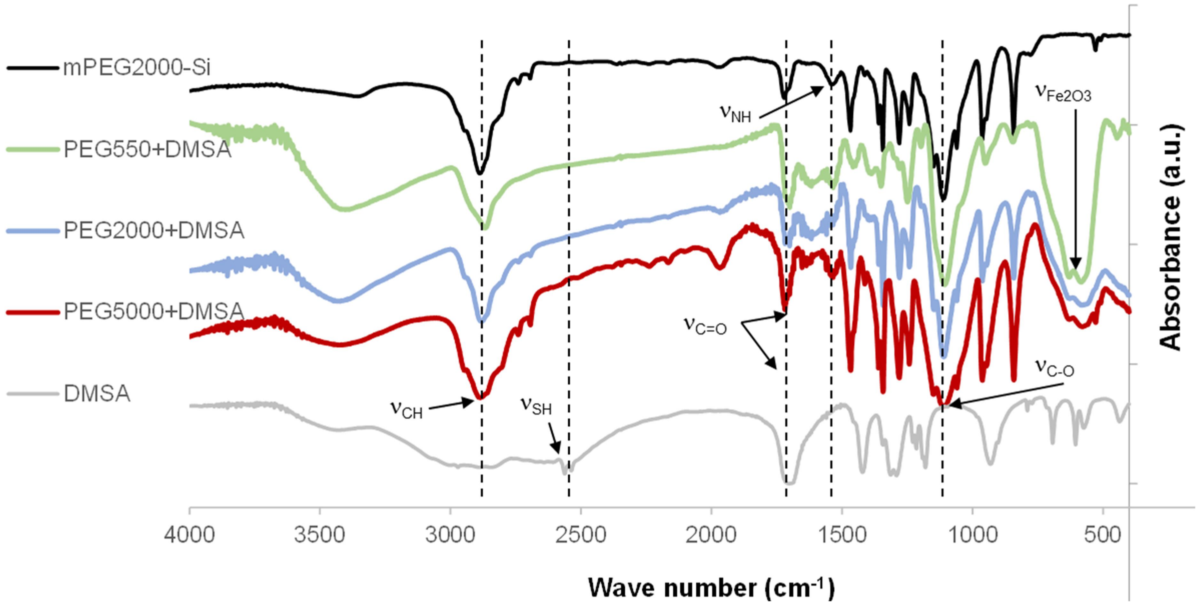

Figure 3: FTIR analyses of naked SPION, mPEG$_{2000}$-Si, mPEG$_{2000}$-Si-SPION-DMSA washed with dialysis and conserved in acidic conditions and DMSA

Figure 3 shows the IR analysis of elaborated nanohybrids as well as that of the pure grafted molecules. In this figure, the presence of the spinel characteristic band at 600-800 cm^{-1} is noted. IR spectra illustrate the DMSA and PEG grafting onto SPIONs surface through the presence of their characteristic bands in nanohybrids spectra. Indeed, the bands at 1120, 2900 and 1500cm^{-1}, reveal mPEG-Si grafting and they are observed for all elaborated nanohybrids with different PEG chains. As mentioned in the previous part, there are two types of νC=O band vibrations at two positions: 1650 cm^{-1} in DMSA and 1720 cm^{-1} in mPEG$_x$-Si. Given that these two positions are close, it is not possible to identify to which molecule the observed band can be attributed to. Thiol characteristic vibration band is absent in the range between 2500 and 2600 cm^{-1}. Taking into account the molecular weight difference between the DMSA and PEG, the latter result could be explained by bands overlap of the two molecules signal which makes the identification of DMSA difficult. Consequently, in this case, IR spectroscopy cannot be a suitable method for the identification of DMSA. Thus, a supplementary technique should be used to confirm the grafting of the two molecules.

XPS elementary analyses of elaborated nanohybrids were carried out. Table 2 shows the atomic percentages of the detected chemical elements: iron (Fe2p), carbon (C1s), oxygen (O1s), silicon (Si1s), nitrogen (N1s) and sulfur (S1s). Detailed information about C1s and O1s XPS spectra decomposition are given in Figure 4 and the atomic concentrations are summarized in Table SI1.

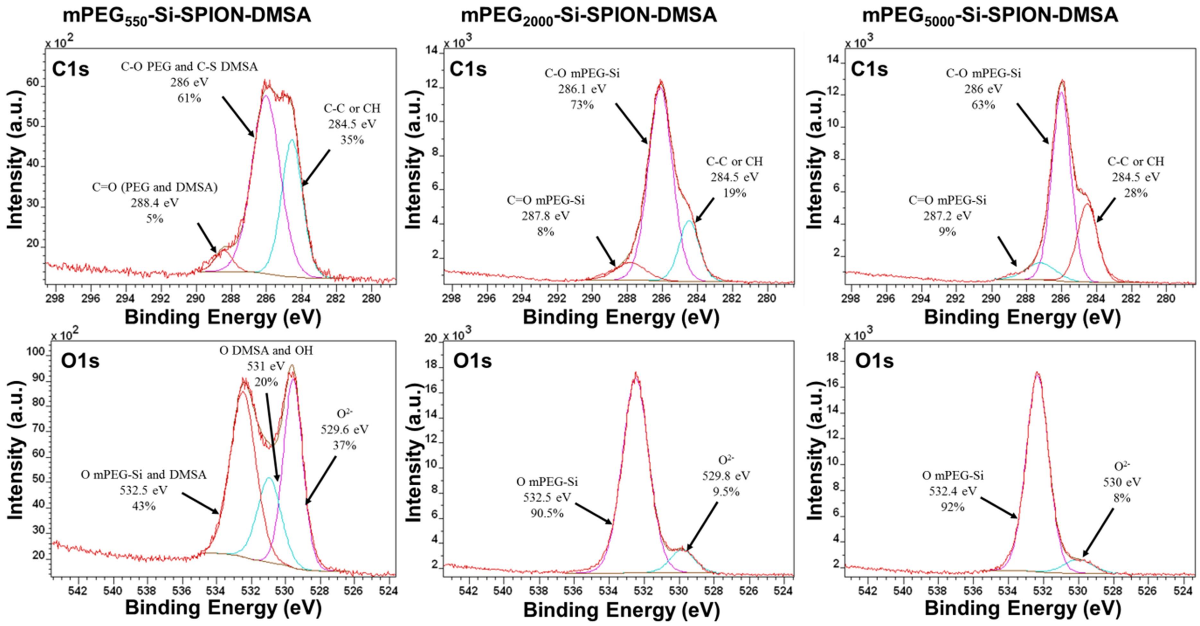

Figure 4: C1s and O1s XPS spectra of mPEG$_X$-Si-SPION-DMSA (x= 550, 2000 or 5000 g.mol^{-1})

The estimation of the grafted molecules quantity onto SPION surface has been realized and an example of calculation for mPEG$_{2000}$-Si-SPION-DMSA is described below. As hypothesis we are assuming that if we measured the contribution of iron, the whole surface functionalization is analyzed. Secondly, we are also assuming that the stoichiometry observed on bare molecules is still valid when they are grafted to iron oxide surface.

For example, in the case of mPEG$_{2000}$-Si-SPION-DMSA, the atomic concentration is as following: carbon (63.8%), oxygen (32.5%), iron (1.45%), nitrogen (1.1%), silicon (1.0%) and sulfur (0.15%). The sulfur percentage allows estimating the ratio DMSA / mPEG$_{2000}$-Si. Figure 4 shows two components in the O1s peak of mPEG$_{2000}$-Si-SPION-DMSA sample. One of them is at 529.6 eV and attributed to O^{2-} of the inorganic core with a contribution of 9.5%.

The second is at 532.2 eV, assigned to C-O-C (90.5%) in $mPEG_{2000}$-Si-DMSA nanohybrid because it is the major bond present in this sample. Indeed, with a sulfur percentage of about 0.15%, the oxygen percentage, coming from DMSA molecule, should be 0.3% (2 sulfurs for 4 oxygens). This percentage is negligible compared to the total percentage of the organic oxygen present in mPEG-Si-SPION-DMSA sample which is 29.4% (90.5%×32.5%). This result confirms the previous hypothesis about the dominance of PEG oxygen in the signal of organic oxygen with 29.1% (29.4%-0. 3%).

The decomposition of C1s peak reveals the presence of three contributions; the first is at 284.5 eV (19.0%) and assigned to carbon from pollution and C-C /C-H bonds. The second is situated at 286.2 eV (73.0%) and attributed to C-O in PEG and C-S in DMSA. The last contribution is shifted to 288.2 eV (8.0%) and can be attributed to N-C=O bond in PEG and O-C=O bond in DMSA. Since the ratio O1s/C1s in $mPEG_x$-Si molecule is 2, the carbon contribution of $mPEG_x$-Si should be 58.2% (29.1%×2). The O1s/C1s ratio in DMSA is 1, so the carbon contribution of DMSA is also 0.4%. As the total carbon percentage is 63.8%, the amount of carbon from pollution is 5.3% (63.8-(0.3+58.2)%). With the same method, the quantification of DMSA and PEG was carried out for the three studied nanohybrids and summarized in Table 2.

Table 2: XPS analysis of elaborated nanohybrids $mPEG_x$-Si-SPION-DMSA (where x = 550, 2000 or 5000 $g.mol^{-1}$) given in atomic concentrations (%).

Element / Sample	O1s			Fe2p	C1s			S1s	N1s	Si2p
	SPION	PEG	DMSA		SPION	PEG	DMSA			
$mPEG_{550}$-Si-SPION-DMSA	14.3	21.4	3.1	7.4	2.35	42.6	3.1	1.55	1.6	2.6
$mPEG_{2000}$-Si-SPION-DMSA	3.1	29.1	0.3	1.45	5.3	58.2	0.3	0.15	1.1	1.0
$mPEG_{5000}$-Si-SPION-DMSA	2.4	27.3	0.3	1.25	12.4	54.6	0.3	0.15	0.7	0.6

Table 2 shows that Fe2p proportion decreases drastically with the increase of the molecular weight of the mPEG-Si. This means that the covering of SPION with PEG is effective. For $mPEG_{550}$-Si-SPION-DMSA nanohybrid, silicon percentage is slightly higher than that of nitrogen. This may be explained by the breaking of some carbamate bonds during the grafting process. For summary, the presence of sulfur demonstrates the presence of DMSA on the PEGylated-SPION and the highest amount is recorded for $mPEG_{550}$-Si-SPION-DMSA sample. For the rest of this part, $mPEG_x$-Si will be determined thanks to nitrogen percentage and DMSA thanks to sulfur one. The number of nitrogen atoms will be considered as the same than that of $mPEG_x$-Si chain and the sulfur corresponds to ½DMSA.

TGA weight loss and XPS analyses were used to determine the amount of grafted molecules (DMSA and PEG) onto functionalized SPION through the two following formula (1) and (2). The sample $mPEG_{2000}$-Si-SPION-DMSA is taken as example and the calculations are done for 100g of dried nanohybrids:

$$\frac{\frac{0.15\%}{2}}{1.1\%} = \frac{n_{DMSA}}{n_{PEG_{2000}}}$$

$$n_{DMSA} = \frac{(\frac{0.15\%}{2}) \times n_{PEG2000}}{1.1\%} = 0.0682\ n_{PEG_{2000}} \qquad (1)$$

Where n_{PEG} and n_{DMSA} are the mole number of PEG and DMSA respectively.

TGA analyses lead to $m_{molecules} = \%TGA \times 100g$, which is the weight loss of $mPEG_{2000}$-Si-SPION-DMSA for 100g of dried nanohybrids (here 56 %)) corresponding to the degradation of both PEG and DMSA molecules alone; $\Delta m_{PEG_{2000}}$ and Δm_{DMSA} are the weight loss in percentage of $mPEG_{2000}$-Si and DMSA respectively (where $\Delta m_{PEG_{2000}}$ = 98% and Δm_{DMSA} = 98% see Figure SI2).

$$m_{molecules}(g) = n_{PEG_{2000}} \times (M_{PEG_{2000}} \times \Delta m_{PEG_{2000}}) + n_{DMSA} \times (M_{DMSA} \times \Delta m_{DMSA}) = 56\% \times 100g \qquad (2)$$

Where: $M_{PEG_{2000}}$ = 2250 $g.mol^{-1}$ and M_{DMSA} = 182.22 $g.mol^{-1}$.

The combination of (1) and (2) gives the following formula:

$$\mathrm{m_{molecules}}(\mathrm{g})=\mathrm{n}_{PEG_{2000}}\times[(\mathrm{M_{PEG_{2000}}}\times\Delta\mathrm{m_{PEG_{2000}}})+0.0682\times\mathrm{n}_{PEG_{2000}}\times(\mathrm{M_{DMSA}}\times\Delta\mathrm{m_{DMSA}})]$$

Then, in the case of $mPEG_{2000}$-Si-SPION-DMSA:

$$\mathrm{n_{PEG_{2000}}}=\frac{56\mathrm{g}}{[(2250\times 98\%)+0.0682\times 182.22\times 98\%]}=0.02526\ \mathrm{moles}$$

And finally $n_{PEG_{2000}} = 2.56\ 10^{-2}$mole, $n_{DMSA} = 2.1\ 10^{-3}$ mole.

Then we assumed that (100-$m_{molecules}$(g)) is the mass of remaining SPION. In the case of $mPEG_{2000}$-Si-SPION-DMSA there is 44g of SPION, with S_{BET}=110 m².g^{-1}, so a total surface of SPION (S_{SPION}) of 4840 m². Then:

$$\textbf{PEG or DMSA/nm}^2=\frac{\mathbf{n_{PEG\ or\ DMSA}\times 6.02\times 10^{23}}}{\mathbf{S}_{\boldsymbol{SPION}}} \qquad (3)$$

$$\mathrm{PEG/nm^2}=\frac{2.56\times 10^{-2}\times 6.02\times 10^{23}}{4840\times 10^{18}}=3.1\ \mathrm{PEG/nm^2}$$

$$\mathrm{DMSA/nm^2}=\frac{2.1\times 10^{-3}\times 6.02\times 10^{23}}{4840\times 10^{18}}=0.2\ \mathrm{DMSA/nm^2}$$

The results of the DMSA and $mPEG_x$-Si grafting efficiency onto SPION are shown in Table 3.

Table 3: The amount of grafted DMSA and PEG expressed in number of molecule/nm² of SPION, based on equation (1) and (2) and grafting efficiency of DMSA and PEG estimated from comparison to the initial added amount and (DMSA: 2.4 DMSA/nm² and PEG: 7.1 PEG/nm²)

Sample	DMSA/nm²	DMSA grafting efficiency (%)*	PEG/nm²	PEG grafting efficiency (%)*
Naked SPION	-	-	-	-
$mPEG_{550}$-SPION-DMSA	1.4	57	2.9	41
$mPEG_{2000}$-SPION-DMSA	0.2	8.5	3.1	44
$mPEG_{5000}$-SPION-DMSA	0.4	17	3.7	55

* grafting efficiency is the grafted amount/the initial engaged amount

Table 3 shows that the grafting efficiency of PEG increases slightly with the increase of molecular weight from 550 to 5000 g/mol. This increase is related to the increase of the organic matter in the PEG chain; however, it is not proportional to the PEG chain difference. The proportion of PEG added during the reaction was 7.1 $mPEG_x$-Si/nm² close to the number of OH/nm² present on SPION surface (7 OH/nm² [41]) and the amount found is between 2.9 and 3.7 PEG/nm² which means that 44% to 55% of the added PEG was grafted (Table 3). These values are higher than those obtained in literature (1 silane/nm² [42]). The high grafting amount can be attributed to a cross-linking of the silanated PEGs between each other as it is usually observed with silica precursors [43].

Table 3 shows also an irregular evolution of DMSA grafting which decreases significantly (about 4 to 7 times) with the increase of grafted PEG chain from 550 to 2000 or 5000 $g.mol^{-1}$. The evolution of the sizes of the polymers could explain these results. For the small $mPEG_{550}$-Si, the low amount of repeating units (12) increases the probability of the polymer to stay in a stretched and elongated configuration compared to bigger mPEG-Si (44 and 112 repeating units) which have more chance to be coiled and to have more interactions with the surface of the SPION [44, 45]. Because of these properties, the longer PEG ($mPEG_{2000}$-Si and $mPEG_{5000}$-Si) could cover more surface area and then prevent the interactions of DMSA with this surface. A schematic explanation is presented on Figure 5.

Figure 5: Explicative scheme of the conjointly grafting of $mPEG_x$-Si (where x = 550, 2000 or 5000 $g.mol^{-1}$) and DMSA on the surface of SPION (grey: mPEG-Si molecules, red: DMSA molecules). With $mPEG_{2000}$-Si and $mPEG_{5000}$-Si, the polymers are bigger and could cover more surface area, preventing their interactions with DMSA.

Conclusion

Through this work, it was possible to quantify for the first time, the amount of a complex mixture of molecules, here DMSA and PEG polymer, grafted onto the surface of SPION in order to enhance their colloidal stability and biocompatibility for further biomedical applications. Different molecular weights of PEG polymer were used for SPION grafting (550, 2000 and 5000 $g.mol^{-1}$) and several techniques were used for nanohybrids characterization. In particular, the accurate chemical composition of the obtained nanohybrids was determined using an original and detailed study based on both XPS elementary analysis and TGA, to quantify the amount of grafted molecules. The obtained results showed a good agreement between the measured and the theoretical compositions of the organic matter before and after grafting. It was also possible to estimate the proportion of each atom onto SPION surface and consequently the grafting rates which is measured between 2.9 and 3.7 PEG/nm^2. This value proves that the mPEG-Si chains cross-link at the surface of the SPION and make a kind of polymer layers surrounding the nanoparticles. The amount of grafted DMSA was also estimated to be in the range between 0.2-1.4 DMSA/nm^2.

These graftings combined a steric repulsion, and a change of the global surface charge from neutral to negative they also lead to thiols groups at the surface of SPION for further functionalizations.

Bibliography

1. T. Neuberger, B. Schopf, H. Hofmann, M. Hofmann, and B. von Rechenberg, J. Magn. Magn. Mater. 293, 483 (2005)
2. L. Maurizi, A.-L. Papa, L. Dumont, F. Bouyer, P. Walker, D. Vandroux, and N. Millot, Journal of Biomedical Nanotechnology 11, 126 (2015)
3. M. Kallumadil, M. Tada, T. Nakagawa, M. Abe, P. Southern, and Q.A. Pankhurst, J. Magn. Magn. Mater. 321, 3650 (2009)
4. Z.L. Zhang, R. Dharmakumar, N. Mascheri, Z.Y. Fan, S.Y. Wu, and D.B. Li, Mol. Imaging 8, 148 (2009)
5. G. Thomas, F. Demoisson, R. Chassagnon, E. Popova, and N. Millot, Nanotechnology 27, 135604 (2016)
6. M. Chastellain, A. Petri, A. Gupta, K.v. Rao, and H. Hofmann, Advanced Engineering Materials 6, 235 (2004)
7. G.S. Demirer, A.C. Okur, and S. Kizilel, J. Mater. Chem. B 3, 7831 (2015)
8. J.L. Dormann, D. Fiorani, and E. Tronc, Adv. Chem. Phys. 98, 283 (1997)
9. Z.Y. Ma, Y.P. Guan, and H.Z. Liu, J. Magn. Magn. Mater. 301, 469 (2006)
10. C.M. Cheng, G. Kou, X.L. Wang, S.H. Wang, H.C. Gu, and Y.J. Guo, J. Magn. Magn. Mater. 321, 2663 (2009)
11. L. Maurizi, F. Bouyer, J. Paris, F. Demoisson, L. Saviot, and N. Millot, Chem. Commun. 47, 11706 (2011)
12. T.J. Daou, S. Begin-Colin, J.M. Greneche, F. Thomas, A. Derory, P. Bernhardt, P. Legare, and G. Pourroy, Chem. Mater. 19, 4494 (2007)
13. G. Thomas, F. Demoisson, J. Boudon, and N. Millot, Dalton Trans. 45, 10821 (2016)
14. X.F. Xue, K. Hanna, C. Despas, F. Wu, and N.S. Deng, J. Mol. Catal. A-Chem. 311, 29 (2009)
15. A. Shkilnyy, E. Munnier, K. Herve, M. Souce, R. Benoit, S. Cohen-Jonathan, P. Limelette, M.L. Saboungi, P. Dubois, and I. Chourpa, J. Phys. Chem. C 114, 5850 (2010)
16. E.A. Vermeij, M.I. Koenders, M.B. Bennink, L.A. Crowe, L. Maurizi, J.-P. Vallée, H. Hofmann, W.B. van den Berg, P.L.E.M. van Lent, and F.A.J. van de Loo, PLoS ONE 10, e0126687 (2015)
17. C. Barrera, A.P. Herrera, and C. Rinaldi, J. Colloid Interface Sci. 329, 107 (2009)
18. J. Salaklang, B. Steitz, A. Finka, C.P.O. Neil, M. Moniatte, A.J.V.d. Vlies, T.D. Giorgio, H. Hofmann, J.A. Hubbell, and A. Petri-Fink, Angew. Chem. Int. Ed. 47, 7857 (2008)
19. P. Perriat, E. Fries, N. Millot, and B. Domenichini, Solid State Ion. 117, 175 (1999)
20. B. Erdem, R.A. Hunsicker, G.W. Simmons, E.D. Sudol, V.L. Dimonie, and M.S. El-Aasser, Langmuir 17, 2664 (2001)
21. F. Sallem, R. Chassagnon, A. Megriche, M. El Maaoui, and N. Millot, J. Alloy. Compd. 722, 785 (2017)
22. G. Thomas, F. Demoisson, O. Heintz, N. Geoffroy, L. Saviot, and N. Millot, RSC Adv. 5, 78614 (2015)
23. F. Bernard, J. Lorimier, V. Nivoix, N. Millot, P. Perriat, B. Gillot, J.F. Berar, and J.C. Niepce, Journal of Solid State Chemistry 141, 105 (1998)
24. D. Aymes, N. Millot, V. Nivoix, P. Perriat, and B. Gillot, Solid State Ion. 101, 261 (1997)
25. F. Bertorelle, C. Wilhelm, J. Roger, F. Gazeau, C. Menager, and V. Cabuil, Langmuir 22, 5385 (2006)
26. C. Oh, Y.G. Lee, T.S. Choi, C.U. Jon, and S.G. Oh, Colloids Surf., A 349, 145 (2009)

27. R. Massart, IEEE Trans. Magn. MAG-17, 1247 (1981)
28. R. Massart, E. Dubois, V. Cabuil, and E. Hasmonay, J. Magn. Magn. Mater. 149, 1 (1995)
29. S. Jo and K. Park, Biomaterials 21, 605 (2000)
30. L. Maurizi, H. Bisht, F. Bouyer, and N. Millot, Langmuir 25, 8857 (2009)
31. C. Flesch, M. Joubert, E. Bourgeat-Lami, S. Mornet, E. Duguet, C. Delaite, and P. Dumas, Colloids Surf., A 262, 150 (2005)
32. R. Shen, P.H.C. Camargo, Y. Xia, and H. Yang, Langmuir 24, 11189 (2008)
33. N. Guigue-Millot, S. Begin-Colin, Y. Champion, M.J. Hytch, G. Le Caer, and P. Perriat, Journal of Solid State Chemistry 170, 30 (2003)
34. S.D. Rolle, D.V. Konev, C.H. Devillers, K.V. Lizgina, D. Lucas, C. Stern, F. Herbst, O. Heintz, and M.A. Vorotyntsev, Electrochim. Acta 204, 276 (2016)
35. P. Poix, Bull. Soc. Chim. Fr. 1085 (1965)
36. T. Belin, N. Guigue-Millot, T. Caillot, D. Aymes, and J.C. Niepce, Journal of Solid State Chemistry 163, 459 (2002)
37. E. Pretsch, P. Buhlmann, and C. Affolter, in *Structure determination of organic compounds* edited Springer, New York (2000), p433.
38. S.M. Montemayor, L.A. Garcia-Cerda, J.R. Torres-Lubian, and O.S. Rodriguez-Fernandez, Mater. Res. Bull. 43, 1112 (2008)
39. Y. Zhang, N. Kohler, and M.Q. Zhang, Biomaterials 23, 1553 (2002)
40. Z.P. Chen, Y. Zhang, S. Zhang, J.G. Xia, J.W. Liu, K. Xu, and N. Gu, Colloids Surf., A 316, 210 (2008)
41. J. Boudon, J. Paris, Y. Bernhard, E. Popova, R.A. Decreau, and N. Millot, Chem. Commun. 49, 7394 (2013)
42. M.D. Butterworth, L. Illum, and S.S. Davis, Colloids Surf., A 179, 93 (2001)
43. L. Maurizi, U. Sakulkhu, L.A. Crowe, V.M. Dao, N. Leclaire, J.-P. Vallée, and H. Hofmann, RSC Adv. 4, 11142 (2014)
44. A. Kyrychenko, D.A. Pasko, and O.N. Kalugin, Phys. Chem. Chem. Phys. 19, 8742 (2017)
45. S.J. Budijono, B. Russ, W. Saad, D.H. Adamson, and R.K. Prud'homme, Colloids Surf., A 360, 105 (2010)

Supplementary information

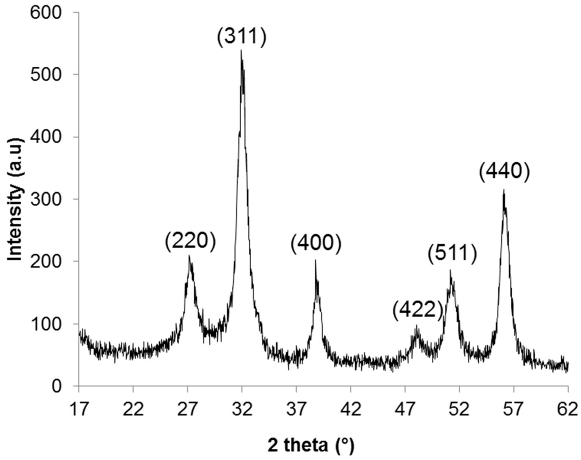

Figure SI1: X-Ray Diffractogram of the naked SPION (K_β from cupper at 1.3922 Å)

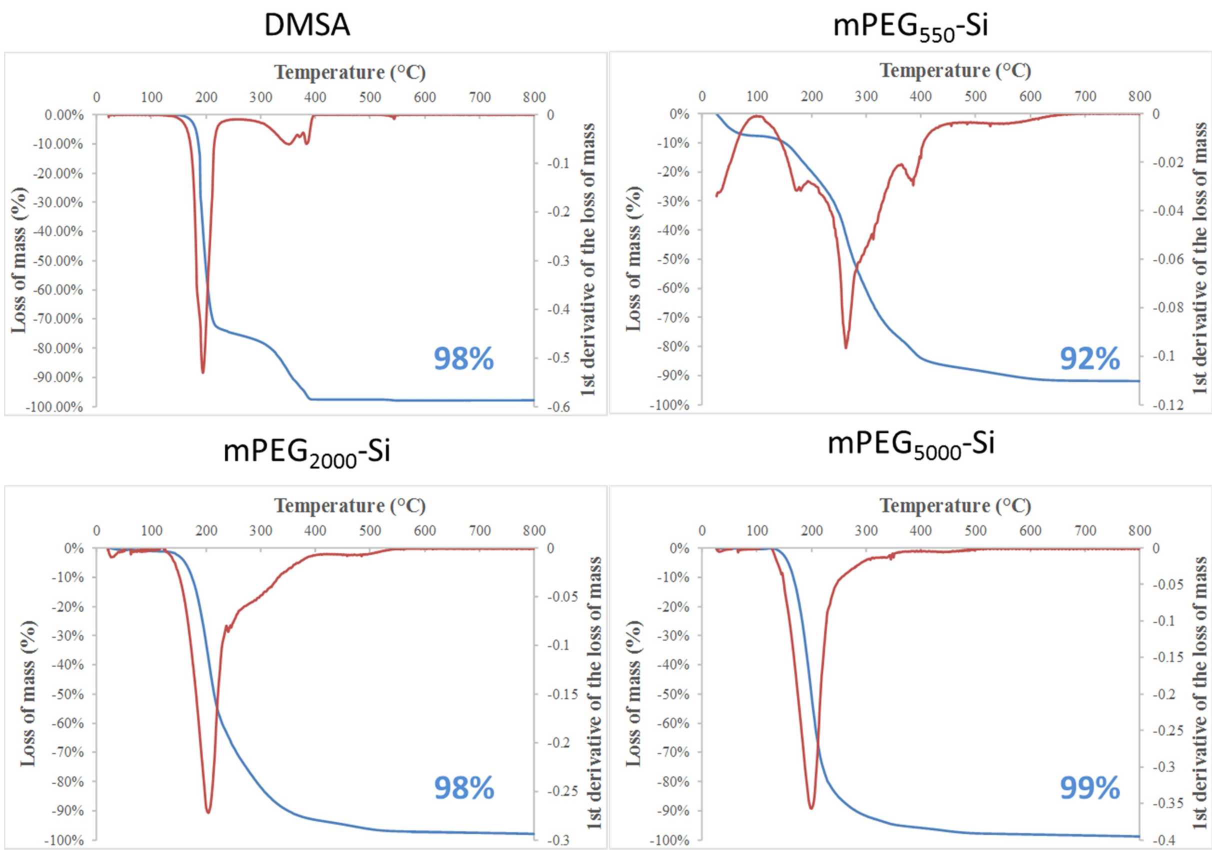

Figure SI2: Thermogravimetric analyses of DMSA and mPEGx-Si (where x = 550, 2000 and or 5000 g.mol^{-1})

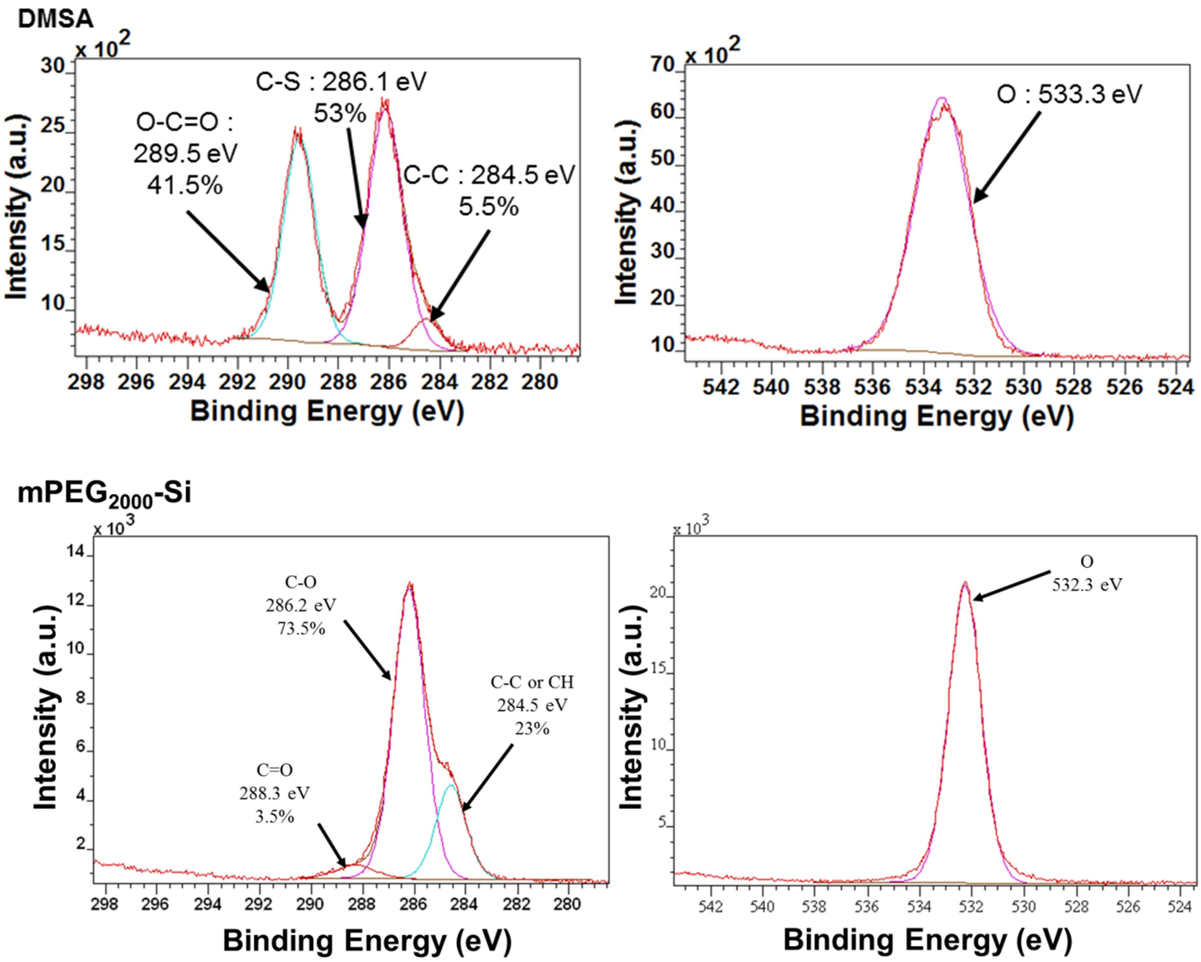

Figure SI3: C1s and O1s XPS of DMSA and mPEG$_{2000}$-Si

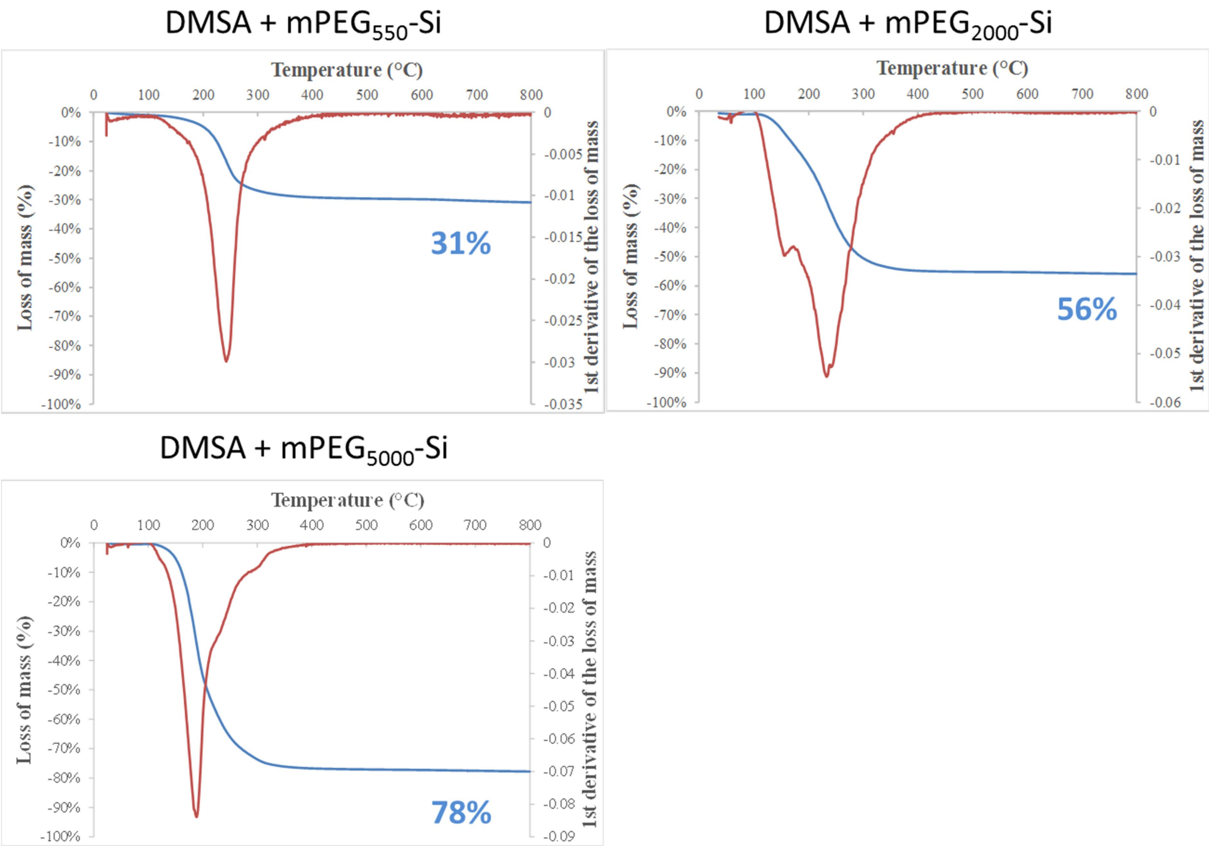

Figure SI4: Thermogravimetric analyses of SPION coated DMSA and mPEGx-Si (where x = 550, 2000 and or 5000 g.mol^{-1})

Table SI1: Atomic concentration of elaborated mPEG$_X$-Si-SPION-DMSA nanohybrids (x = 550, 2000 or 5000 g.mol^{-1})

Elements (%)	Fe2p	C1s	O1s	Si1s	N1s	S1s
mPEG$_{550}$-SPION-DMSA	7.4	48.1	38.7	2.6	1.6	1.55
mPEG$_{2000}$-SPION-DMSA	1.45	63.8	32.5	1.0	1.1	0.15
mPEG$_{5000}$-SPION-DMSA	1.25	67.3	30.0	0.6	0.7	0.15

Graphical abstract

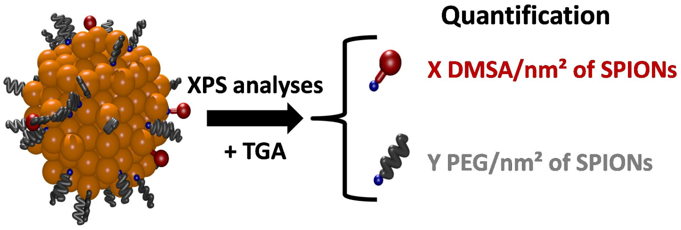

One step co-functionalization of SPIONs with DMSA and PEG: by coupling thermogravimetric to X-Ray photoelectron spectrometry analyses it was possible to quantify accurately the covering of nanoparticle's surface.